QUARTERLY OF APPLIED MATHEMATICS
VOLUME LXVI, NUMBER 3
SEPTEMBER 2008, PAGES 447–471
S 0033-569X(08)01093-3
Article electronically published on June 4, 2008

INFLUENCE OF SUCTION/BLOWING ON THE FINITE AMPLITUDE DISTURBANCES HAVING NON-STATIONARY MODES OF A COMPRESSIBLE BOUNDARY LAYER FLOW

By

M. TURKYILMAZOGLU

Department of Mathematics, Hacettepe University, 06532-Beytepe, Ankara, Turkey

Abstract. In this paper, a weakly non-linear stability analysis is pursued to explore the effects of suction and blowing on a compressible mode of instability of the three-dimensional boundary layer flow induced by a rotating disk. The main thrust of the research is to extend the stationary work of Seddougui and Bassom (1996) to cover for the non-stationary mode so that it is targeted to determine whether the major role in finite amplitude destabilization of the boundary layer is played by the stationary mode of Seddougui and Bassom (1996) or the non-stationary mode as calculated from the present study. Within this perspective, the basic compressible flow obtained in the large Reynolds number limit, together with a suction parameter entering into the wall with normal velocity at the wall, is perturbed by disturbances which are constituted as the non-linear interaction of fundamental modes and harmonics. The effects of non-linearity are then explored by deriving a finite amplitude equation governing the evolution of the non-linear lower branch modes and also allowing the finite amplitude growth of a disturbance close to the neutral location determined from a prior stability analysis. Although the form of the amplitude equation is not at all surprising (given a similar result for the stationary vortices in Seddougui and Bassom (1996)), the dependence of the coefficients of the Landau-type modulated vortex amplitude equation on the frequency parameter is established here. A close examination of the coefficients of this evolution equation indicates strongly that the non-linearity has a destabilizing effect for both suction and blowing through the surface of the disk, the effect of which is much more stronger for a suction. Also the impact of non-linearity is higher for the non-stationary compressible modes than for the stationary waves of Seddougui (1990) and Seddougui and Bassom (1996). Moreover, in the case of suction, there occurs a regime of non-stationary modes that cover not only the positive frequency waves, but also waves having negative frequencies, and these modes are always unstable no matter whether the wall is insulated

Received January 22, 2007.
2000 *Mathematics Subject Classification.* Primary 76U05; Secondary 76E09, 34K25.
Key words and phrases. Rotating-disk flow, suction/blowing, linear/non-linear waves, compressible boundary layer.
E-mail address: turkyilm@hotmail.com

or isothermal. The solution of the asymptotic amplitude equation further demonstrates that as the local Mach number increases, compressibility has the influence of stabilization by requiring smaller initial amplitude of the disturbance for the laminar rotating disk boundary layer flow to become unstable whenever fluid injection is applied. Unlike this, suction makes the underlying flow more convectively unstable as far as the compressibility is concerned, particulary for the modes generated as a consequence of an isothermal wall. Both for the suction and injection cases, disturbances having positive frequency are always shown to cause an instantaneous non-linear amplification prior to the negative frequency waves.

1. Introduction. In the present study, we consider the compressible boundary layer flow on a rotating disk and its non-linear instability owing to the existence of three-dimensional crossflow vortices pertaining to this flow. The subject is of great significance in order to know the precise effects of heating/cooling of the wall together with suction/blowing through the surface of the wall, due to the reason that these may enable us to keep the flow over aeronautical vehicles laminar or at least to delay the occurrence of turbulence. Among the many instability mechanisms taking place over two- and three-dimensional boundary layer flows, crossflow instability has received a great deal of attention. The crossflow-type instability is mainly attributed to the inflectional nature of the steady mean flow profile known as the Von Karman's exact similarity solution in the case of incompressible rotating-disk flow. This instability is known to give rise to linear as well as to the finite amplitude destabilization of the three-dimensional boundary layers. Therefore, the interest in the instability investigations of rotating disk boundary layer flow has increased outstandingly both in terms of experimental and theoretical means.

The research conducted so far on the flow due to a rotating disk hints that the underlying crossflow vortex instability is a result of either absolute instability or convective types of instability. The absolute instability is a linear one studied first in [3] and [4]. These studies, together with later investigations in [5, 6] and [7, 8, 9, 10], have proven that the infinite growth of the unstable disturbances in the radial directions may be a reason for transition in rotating disk flow. On the other hand, the surface coating suggested in [11] or the suction through the wall as applied in [12] and [13] may effectively delay the occurrence of absolute instability.

The early research conducted in [14] shows that the crossflow instability manifests itself in the form of a viscous lower branch or an inviscid upper branch. The fundamental features of these modes were enlightened both experimentally and theoretically by many researchers; among them include [7], [15, 16, 17], [18], [19, 20], [21], [22], [23], [24]. These investigations clearly showed that the inviscid instability is characterized by the form of a stationary pattern due to the superposition of modes of zero-frequency spiral vortices, which aligned themselves at an inclination angle of almost 13° normal to the radius vector. Numerical evaluations predict a critical Reynolds number of about 300 for the onset of amplification through the inviscid instability. Moreover, investigations also showed the existence of viscous instability that occurred with a much lower critical transition Reynolds number, readily depending on the frequency, than the inviscid stationary mode. This instability, which was also observed experimentally in [23], manifests itself as a wave

pattern of spiral vortices inclined at a higher angle, of about 20°, to the radius vector with a lower wavenumber than that corresponding to the inviscid instability of [14].

Both the absolute instability and convective instability results from the references cited above were based on the linear stability theory together with a classical parallel flow approximation employed to simplify the governing stability equations. Later investigations were based on a more rational approach accounting for the non-linearity and non-parallelism of the basic flow, with a large Reynolds number asymptotic approximation. This method is known as the triple deck theory, which was first used within the context of predicting the stability features of Blasius boundary layer flow in [29] and [30]. See [25, 26], [27] and [28] for the description and its applications. This strategy was first applied to the rotating disk flow in [31] in which both upper branch and lower branch stationary neutral modes and their asymptotic structures were obtained within the framework of asymptotic expansion at large Reynolds numbers. It was shown that the lower branch corresponds to an effective velocity profile having zero shear stress at the surface of the disk. Making use of the asymptotic triple deck theory, the linear and non-linear evolution of upper branch modes of the rotating disk boundary layer flow, as far as the orientation of the non-stationary waves are concerned, were examined in [32] and [33]. These modes are the ones naturally observed in the experiments of [14], [20] and [34, 35]. However, as first detected in the experiment of [23], there exists lower branch modes corresponding to a lower Reynolds number. [36] investigated, making use of the theory set up in [31], the non-linear stability properties of lower branch stationary modes. [36] found that non-linearity destabilizes these modes which are also shown to be amenable to subcritical instability, and for these unstable modes to be seen experimentally, the system must be strongly forced; otherwise the dominant inviscid modes of [14] would be normally observed. The existence of a subcritical instability was also confirmed by the experimental results given in [37, 38].

The non-linear incompressible work of [36] was extended in [2] to incorporate the effects of compressibility on the stationary modes. [2] found that the lower branch modes could only be possible for a finite range of Mach numbers, and the threshold amplitude beyond which the instability may persist is significantly reduced when the surface of the disk is highly cooled. A further extension of [36] to include the non-stationary lower branch modes has been recently implemented in [39], in which the compressibility effects on the evolution of linear modes were investigated. Non-linearity has been taken into account in [40], and it was shown that a smaller initial finite amplitude of the disturbance with a positive frequency is sufficient to give rise to an exponential growth of the lower branch non-stationary modes, which would then cause the transition to turbulence in the rotating disk boundary layer flow, of course in the absence of other dominant instability mechanisms. The impacts of applying suction or injection through the disk surface were discussed for the absolute instability in the work of [13] and for the convective instability in the works of [12] and [1], but these were limited to the case of the incompressible Von Karman's boundary layer flow. Motivated by the latter works, we in the present study aim to study the influences of not only the compressibility but also the mass transfer on the lower branch non-stationary neutral modes as studied in the case of zero-suction in [39]. Thus, a comparison between the stationary modes of [1] and the non-stationary

modes as calculated here can be done to understand the importance. However, the present work is more involved due to the fact that applying suction/injection on the wall couples the basic velocity profiles to the energy equation through a wall temperature parameter, which is neither the case for the incompressible flow with suction as in [12] nor the case for the compressible zero-suction as in [39]. An amplitude equation has been obtained, whose coefficients imply that the non-linearity has a finite amplitude destabilization on the lower branch modes for both suction and blowing applied at the disk. The modes under compressible effects with suction are more subjected to instability. Regardless of whether the adiabatic or isothermal wall conditions are considered, there exists a region of positive frequencies (and also negative frequencies for the modes under strong wall cooling with suction) that are always unstable. Moreover, much less initial amplitude disturbance is sufficient than for that of the stationary modes determined in [2] and [1], if the perturbations have positive frequencies, an outcome that is also in line with that of [40]. In addition to this, the appearance of double modes for the lower branch curves having positive frequencies as encountered in the numerical stability solution of non-stationary incompressible flow in [24] is clarified here, whose interval of occurrence is particularly increased in the case of suction but reduced in the presence of wall cooling together with injection.

The following strategy is adopted for the rest of the paper. In §2.1 the non-linear partial differential equations governing the stability of the compressible boundary layer flow over a rotating disk are given together with the generalized basic Von Karman's steady flow including the suction/blowing on the disk surface. §3 involves the construction of a triple-deck structure of the disturbed flow. The significant terms in the wall layer region are derived, and using a solvability condition on the linear lower-deck problem, an eigenrelation is generated among the effective wavenumber, wave angle and frequency. Perturbing the solution near the neutral location, an equation for the disturbance amplitude is obtained that presents the finite amplitude effects due to the non-linear terms. The impacts of mass transfer on the linear results are first briefly discussed in §4.1, followed by the weakly non-linear finite amplitude discussions in §4.2. Conclusions are finally drawn in §5.

2. Problem formulation.

2.1. *Governing equations.* We are concerned here with the unsteady flow of a compressible viscous fluid over an infinite disk rotating with constant angular velocity Ω_a about the axial axis z. Having suitably non-dimensionalized the flow variables in the rotating frame in terms of cylindrical polar coordinates (r, θ, z) possessing an orthonormal unit base $(\hat{r}, \hat{\theta}, \hat{k})$, the non-dimensional velocities $\mathbf{u} = (u, v, w)$, the pressure p, the density ρ, and the temperature T are governed by the following continuity, momentum,

state, and energy equations:

$$\frac{\partial \rho}{\partial t} + \nabla \cdot (\rho \mathbf{u}) = 0, \tag{2.1}$$

$$\rho\big[\frac{\partial \mathbf{u}}{\partial t} + (\mathbf{u}\cdot\nabla)\mathbf{u} + 2(\hat{k}\times\mathbf{u}) - \mathrm{r}\hat{r}\big] = -\nabla p + \frac{1}{R}\big[\nabla(\lambda\nabla\cdot\mathbf{u}) + \nabla(\mu e_{ij})\big], \tag{2.2}$$

$$\Gamma M_\infty^2 p = \rho T, \tag{2.3}$$

$$\begin{aligned}\rho\big[\tfrac{\partial T}{\partial t} + (\mathbf{u}\cdot\nabla)T\big] &= M_\infty^2(\Gamma-1)\big[\tfrac{\partial p}{\partial t} + (\mathbf{u}\cdot\nabla)p\big] + \tfrac{1}{R}\nabla\cdot(k\nabla T)\\ &+\tfrac{\Gamma-1}{R}M_\infty^2\big[\tfrac{1}{2}\mu\Psi^2 + \lambda(\nabla\cdot\mathbf{u})^2\big].\end{aligned} \tag{2.4}$$

Here, e_{ij} denote the strain tensors, and μ and λ are the shear and bulk viscosities of the fluid, respectively. Moreover, R defines the characteristic Reynolds number given by $R = \Omega_a l^2 \frac{\rho_\infty}{\mu_\infty}$, in which l is some reference length, for instance the local radius of the disc, and ρ_∞ and μ_∞ are the free-stream values of the density and shear viscosity of the fluid, respectively, which were used to make the flow variables non-dimensional. The equation of state (2.3) shows that the fluid considered is a perfect gas, whose ratio of the specific heat is represented by $\Gamma = c_p/c_v$, where c_p is the specific heat at constant pressure and c_v is the specific heat at constant volume. The free-stream Mach number is given by $M_\infty = \frac{\Omega_a l}{\sqrt{\Gamma \Re T_\infty}}$, where T_∞ is the free-stream temperature and $\Re$ is the gas constant, which can be expressed as the difference of c_p and c_v. Further, the parameter k appearing in equation (2.4) is the coefficient of thermal diffusivity that is related to the Prandtl number σ by $\sigma = \frac{\mu}{k}$. Finally, Ψ is a dissipation function associated with the strain tensors and is given, for instance, in [39], but the details of this quantity as well as the second coefficient of viscosity λ are not required for the following analysis.

2.2. *The basic flow.* To obtain the steady compressible flow equations of motion, which are known as the Von Karman's similarity solution in the case of incompressible zero-suction, equations (2.1–2.4) must be supplemented with the no-slip boundary conditions on the wall except with suction/injection permitted on the wall with normal velocity through a scaled parameter $\bar{s}$ such that $\bar{s} > 0$ is to denote the suction and $\bar{s} < 0$ denotes the blowing applied to the flow at the surface of the disk. Additionally, no motion far away from the disk should be allowed. Furthermore, we have a freedom on the choice of the boundary condition for the temperature at the disk surface. Either the disk can be considered as thermally insulated (adiabatic surface), that is,

$$\frac{\partial T}{\partial z} = 0 \quad \text{at} \quad z = 0,$$

or we have a prescribed value of temperature at the wall (isothermal wall), that is,

$$T = T_w \quad \text{at} \quad z = 0.$$

The density and temperature approach their free-stream values of unity as $z \to \infty$.

In what follows, the Reynolds number will be taken to be large, and since the boundary layer thickness is $O(R^{-1/2})$, the steady compressible boundary layer flow over a rotating-disk evolves along a boundary layer coordinate of order unity, defined by $\bar{Y} = R^{1/2}z$. In order to remove the basic density term $\bar{\rho}$ from the equations of motion, the Dorodnitsyn-Howarth transformation (see for example [41]) is made with the introduction of a new

coordinate $y = \int_0^{\bar{Y}} \bar{\rho} d\bar{Y}$. In turn, the idealized Chapman's viscosity law is assumed so that $\mu = CT$, for which C is taken to be unity. Accounting for all of these, the basic velocity profile is represented by

$$\mathbf{u_B} = (r\bar{u}(y), r\bar{v}(y), R^{-1/2}\bar{T}(y)\bar{w}(y)), \tag{2.5}$$

where, for large R, the functions $\bar{u}$, $\bar{v}$, and $\bar{w}$ in (2.5) satisfy

$$\begin{aligned} &\psi'^2 - (\bar{v}+1)^2 - 2\psi\psi'' - \psi''' = 0, \\ &2\psi'(\bar{v}+1) - 2\psi\bar{v}' - \bar{v}'' = 0, \end{aligned} \tag{2.6}$$

for an appropriately defined stream function variable ψ given as $\bar{u} = \psi'$ and $\bar{w} = -2\psi$. Equations (2.6) are to be solved subject to

$$\begin{aligned} &\psi = \tfrac{\bar{s}}{2T_w}, \quad \psi' = 0, \quad \bar{v} = 0, \qquad \text{at } \ y = 0, \\ &\psi' = 0, \qquad \bar{v} = -1, \qquad\qquad \text{as } \ y \to \infty. \end{aligned} \tag{2.7}$$

Within the transformations specified above, it is an easy matter to show that the solution to the energy equation can be written as a linear combination of a heat conduction term f and a viscous dissipation term q (see for instance [42]), such that

$$\bar{T} = \tfrac{1}{\bar{\rho}} = 1 + \tfrac{(\Gamma-1)}{4} M^2 f + (T_w - 1)q, \tag{2.8}$$

in which Γ is assigned to a value of 1.4 for air, $M = rM_\infty$ is the local Mach number, and functions f and q satisfy the ordinary differential equations

$$\begin{aligned} &q'' + 2\sigma\psi q = 0, \\ &f'' + 2\sigma\psi f' - 2\sigma\psi' f = -4\sigma(\psi''^2 + \bar{v}'^2). \end{aligned} \tag{2.9}$$

It should be remarked here that due to the imposition of suction or blowing, the compressible flow equations (2.6) are coupled to the energy equation (2.8–2.9) through the boundary condition (2.7), which is in direct contrast to the case of either a zero-suction or a corresponding incompressible case; see, for example, [39] and [2]. For the particular case of a model fluid with $\sigma = 1$, exact solutions for f and q can be obtained under the boundary conditions on the flow temperature; see, for instance, [7]. However, we shall concentrate on a more ideal fluid here and use $\sigma = 0.72$ throughout in the subsequent analysis. Despite the fact that the selection of the Prandtl number has an influence on the linear and viscous absolutely unstable modes (see for instance [43]), the use of 0.72 as opposed to 1 is believed to have little quantitative effect on our high Reynolds number convective instability results. Two more points are worthy of consideration here. First, if a thermally insulated disk is taken into account, then (2.6–2.9) must be provided with the boundary conditions

$$f'(0) = q'(0) = 0, \qquad f(\infty) = q(\infty) = 0, \tag{2.10}$$

as a consequence of which, the wall temperature from (2.8) is found to be $T_w = 1 + \frac{1}{4}(\Gamma - 1)M^2 f(0)$, indicating that the basic flow variables $\bar{u}$, $\bar{v}$, $\bar{w}$, and f are coupled with a strict dependence on the value of Mach number M. Second, if however an isothermal disk is accounted for, the dependence of the basic velocities on the Mach number is avoided,

but equations (2.6–2.7) and (2.8) are still coupled through the suction parameter $\bar{s}$ and T_w. The boundary conditions on (2.10) in this case become

$$f(0) = q(0) - 1 = 0, \qquad f(\infty) = q(\infty) = 0. \tag{2.11}$$

The first equation in (2.9) can be straightforwardly integrated to get a solution for q. The ensuing analysis requires the values for $\bar{u}'(0)$, $\bar{v}'(0)$, and $f(0)$ for the adiabatic wall conditions and, additionally, $f'(0)$ and $q'(0)$ for heat transfer applied at the surface of the disk, which are numerically calculated and discussed in Section 4.

3. The stability analysis. The mean flow determined from (2.5–2.7) is next perturbed with infinitesimally small disturbances of the form

$$l\Omega_a(\tilde{U}(r,\theta,z,t), \tilde{V}(r,\theta,z,t), \tilde{W}(r,\theta,z,t), \tilde{P}(r,\theta,z,t), \tilde{\rho}(r,\theta,z,t), \tilde{T}(r,\theta,z,t)). \tag{3.1}$$

Having substituted the mean flow (2.5) together with the disturbances (3.1) into the governing equations (2.1–2.4) and subtracting out the basic field, the evolution of the compressible disturbed flow will be governed by a set of non-linear equations which are given in [39] for the linearized case. We are then interested in the asymptotic solutions of the disturbances (3.1) having triple-deck structure and also based on the small parameter ε defined by $\varepsilon = R^{-\frac{1}{16}}$ in the limit of a large Reynolds number. It should be warned that with such a small parameter there is a danger of hitting the absolutely unstable regime, which is avoided here by assuming only the presence of convectively unstable modes. The structure for the stationary lower branch viscous incompressible modes was first described in [31] and [36], which was later extended in [2] to cover for the compressibility effects. The linear asymptotic results incorporating the non-stationary disturbances have been recently presented in [39]. Therefore, in what follows, we omit most of the linear results and focus on the non-linear evolution of the perturbations that evolve under the influence of a suction parameter $\bar{s}$.

The asymptotic three-dimensional solutions of the non-stationary modes of instability in the triple-deck regions, namely upper, main, and lower decks, will be sought proportional to

$$E = e^{(i/\varepsilon^4)(\int^r \alpha(r)dr + \beta\theta - \varepsilon^2\omega t)}, \tag{3.2}$$

and the wavenumbers (α, β) and the frequency ω expand for convenience in terms of the small parameter ε as

$$\begin{aligned} \alpha &= \alpha_0 + \varepsilon^2\alpha_1 + \cdots, \\ \beta &= \beta_0 + \varepsilon^2\beta_1 + \cdots, \\ \omega &= \varepsilon\omega_0 + \varepsilon^3\omega_1 + \cdots. \end{aligned} \tag{3.3}$$

The forms of the expansions of the disturbance will be essentially found by balancing the convection and viscous terms in (2.2). Also, the perturbation terms will be in the form of fundamental terms plus harmonic terms arising from the non-linear nature of the governing equations (2.1–2.4). Here, we search for the local wavenumber and frequency components that contribute to the neutrally stable flow initially at a radial location r. Afterwards, the finite amplitude non-linear solutions close to the location of neutral stability will be considered. Next, following closely the study of [2], the wavenumbers and frequency as given in (3.3) and the disturbances proportional to (3.2) will be substituted

into the Navier-Stokes equations (2.1–2.4), and the solutions to the expansions of the flow quantities will be sought separately in each asymptotic triple-deck region. In fact, to be concise, solutions to the disturbance quantities are first obtained in the upper deck having a thickness of ε^4, which are then matched with the solutions of the main deck having a thickness of ε^8. Solutions in the main deck are also enforced to satisfy the vanishing effective wall shear at the leading order. Up to now, the expansions and solutions are similar to those obtained in [2]. However, differences arise in the lower deck which are required to reduce the slip velocities to zero at the surface of the disk. Thus, we concentrate on the lower-deck region.

In the lower deck, in the large Reynolds number limit, the thickness of the viscous sublayer is given by

$$\zeta = \varepsilon^{-9} z = O(1).$$

The expansion of the basic flow quantities (2.5) in terms of the lower-deck scaling will lead to

$$\begin{array}{l}
\bar{\rho} = R_w + \varepsilon \bar{\rho}_0 \zeta + \cdots, \\
\bar{T} = T_w + \varepsilon \bar{T}_0 \zeta + \cdots, \\
\bar{u} = \varepsilon \frac{\bar{u}_0}{T_w} \zeta + \varepsilon^2 \frac{\bar{u}_1}{T_w^2} \zeta^2 + \cdots, \\
\bar{v} = \varepsilon \frac{\bar{v}_0}{T_w} \zeta + \varepsilon^2 \frac{\bar{v}_1}{T_w^2} \zeta^2 + \cdots, \\
\bar{w} = -\frac{\bar{s}}{T_w} - \varepsilon^2 \bar{u}_0 \zeta^2 - \frac{2}{3} \varepsilon^3 \frac{\bar{u}_1}{T_w} \zeta^3 + \cdots,
\end{array} \tag{3.4}$$

where the coefficients depend on r and come from the Taylor expansion at the wall. Moreover, the condition of zero wall shear can be written as

$$\alpha_0 r \bar{u}_0 + \beta_0 \bar{v}_0 = 0. \tag{3.5}$$

It should be remarked here that equation (3.5) relies heavily on the suction parameter $\bar{s}$, in contrast to the corresponding constant value of 1.207 for the zero-suction compressible flow case.

In order for the solutions to match with those in the main deck as $\zeta \to \infty$, the radial velocity disturbance must have the form

$$\begin{array}{l}
\tilde{U} = \varepsilon^{-1}[r A_1 (\frac{\bar{u}_0}{T_w} + 2\varepsilon \frac{\bar{u}_1}{T_w^2} \zeta + \cdots) + (U_{-1} + \varepsilon U_0 + \cdots)] \delta E \\
+\delta^2 \varepsilon^{-4} \{[r \frac{A_2}{2} (\frac{\bar{u}_0}{T_w} + 2\varepsilon \frac{\bar{u}_1}{T_w^2} \zeta + \cdots) + (U_{20} + \varepsilon U_{21} + \cdots)] E^2 + \varepsilon (U_{m0} + \varepsilon U_{m1} + \cdots)\} \\
+\varepsilon^{-7}[r \frac{A_3}{3} (\frac{\bar{u}_0}{T_w} + 2\varepsilon \frac{\bar{u}_1}{T_w^2} \zeta + \cdots) + (U_{30} + \varepsilon U_{31} + \cdots)] \delta^3 E^3 \\
+\varepsilon^{-7}[r A_4 (\frac{\bar{u}_0}{T_w} + 2\varepsilon \frac{\bar{u}_1}{T_w^2} \zeta + \cdots) + (U_{10} + \varepsilon U_{11} + \cdots)] \delta^3 E + O(\delta^4) + c.c.,
\end{array} \tag{3.6}$$

together with a similar expression for the azimuthal velocity, density, and temperature perturbations, while the normal velocity perturbation $\tilde{W}$ expands as

$$\begin{array}{l}
\tilde{W} = \varepsilon^5 \{-i A_1 [(r\alpha_0 \frac{\bar{u}_1}{T_w^2} + \beta_0 \frac{\bar{v}_1}{T_w^2}) \zeta^2 + \varepsilon (r\alpha_0 \frac{\bar{u}_2}{T_w^3} + \beta_0 \frac{\bar{v}_2}{T_w^3}) \zeta^3 + \cdots] + (\varepsilon W_0 + \cdots)\} \delta E \\
+\delta^2 \varepsilon^2 \{[-i A_2 [(r\alpha_0 \frac{\bar{u}_1}{T_w^2} + \beta_0 \frac{\bar{v}_1}{T_w^2}) \zeta^2 + \varepsilon (r\alpha_0 \frac{\bar{u}_2}{T_w^3} + \beta_0 \frac{\bar{v}_2}{T_w^3}) \zeta^3 + \cdots] + (\varepsilon W_{20} + \cdots)] E^2 \\
+\varepsilon^4 (W_{m0} + \varepsilon W_{m1} + \cdots)\} \\
+\{-i A_3 \varepsilon^{-1} [(r\alpha_0 \frac{\bar{u}_1}{T_w^2} + \beta_0 \frac{\bar{v}_1}{T_w^2}) \zeta^2 + \varepsilon (r\alpha_0 \frac{\bar{u}_2}{T_w^3} + \beta_0 \frac{\bar{v}_2}{T_w^3}) \zeta^3 + \cdots] + (W_{30} + \cdots)\} \delta^3 E^3 \\
+\{-i A_4 \varepsilon^{-1} [(r\alpha_0 \frac{\bar{u}_1}{T_w^2} + \beta_0 \frac{\bar{v}_1}{T_w^2}) \zeta^2 + \varepsilon (r\alpha_0 \frac{\bar{u}_2}{T_w^3} + \beta_0 \frac{\bar{v}_2}{T_w^3}) \zeta^3 + \cdots] + (W_{10} + \cdots)\} \delta^3 E \\
+O(\delta^4) + c.c.,
\end{array} \tag{3.7}$$

and $\tilde{P}$ expands as

$$\begin{aligned}\tilde{P} &= \varepsilon^3(P_0+\varepsilon P_1+\cdots)\delta E+\delta^2[(P_{20}+\varepsilon P_{21}+\cdots)E^2+\varepsilon^{10}(P_{m0}+\varepsilon P_{m1}+\cdots)]\\ &+\varepsilon^{-3}(P_{30}+\varepsilon P_{31}+\cdots)\delta^3E^3+\varepsilon^{-3}(P_{10}+\varepsilon P_{11}+\cdots)\delta^3E+O(\delta^4)+c.c.,\end{aligned} \tag{3.8}$$

where $c.c$ denotes the complex conjugate of a quantity, $A_i=\frac{\gamma C_i}{\beta_0^2}$, $i=1,2,3,4$, and the flow quantities in this region depend on r and ζ. The leading-order effective wavenumber γ is found to be in the upper deck as $\gamma^2=\gamma_0^2-\beta_0^2M_\infty^2$ with $\gamma_0^2=\alpha_0^2+\frac{\beta_0^2}{r^2}$. It is worthy of mentioning here that the compressible non-stationary neutral lower branch disturbances are not confined within specified local Mach numbers as in the zero-suction case ($0\le M\le 1.56$; see [2]), but the interval of existence of the modes depends upon the consideration of suction or blowing; see [1].

After substituting expressions (3.4–3.8) into the non-linear disturbance equations obtained by perturbing (2.1–2.4), equating the same order ε terms from the terms proportional to δE, and also following the arguments given in [2], we obtain the leading-order normal wall velocity disturbance W_0 as

$$\begin{aligned}W_0 &= -iA_1\tfrac{U_{10}}{T_w}\Delta^{-1/4}s+iA_1\omega_0F_1(s)+\{\tfrac{\gamma_0^2}{T_w}CF_2(s)+\tfrac{2}{T_w^3}i\beta_0A_1[1+\tfrac{\bar{v}_0^2}{\bar{u}_0^2}]\tfrac{\bar{u}_0}{U_c(0,0)}F_3(s)\\ &-6A_1\Delta\tfrac{T_w\bar{T}_0}{U_c(0,0)}F_4(s)+A_1(\sigma-1)\Delta\tfrac{T_w^3\bar{\rho}_0}{U_c(0,0)}F_5(s)\}\Delta^{-3/4}+k_1s^2,\end{aligned} \tag{3.9}$$

where $s=\Delta^{1/4}\zeta$, $U_{ij}=(r\alpha_i\bar{u}_j+\beta_i\bar{v}_j)$, $\Delta=\frac{i}{T_w^4}U_{01}$, and k_1 is an arbitrary constant to be found by matching the solution (3.9) to the main-deck solution. The particular solutions F_1, F_2, F_3, F_4, and F_5 in (3.9) satisfy Weber-like (see [44]) differential equations and boundary conditions as also given in [39]. It can also be directly computed from a suitable contour integration that

$$\begin{aligned}I_1&=F_1'(0)=1.3520,\\ I_2&=F_2'(0)=\tfrac{1}{2U_c(0,0)}\textstyle\int_0^\infty\theta U_c(0,\theta)d\theta=0.5990,\\ I_3&=2\tfrac{F_3'(0)}{U_c(0,0)}=\tfrac{1}{U_c^2(0,0)}\textstyle\int_0^\infty\theta U_c^2(0,\theta)d\theta=0.4570,\\ I_4&=F_4'(0)=0.0192,\\ I_5&=F_5'(0)=1.6972,\end{aligned} \tag{3.10}$$

with U_c denoting the parabolic cylinder function; see, for instance, [44]. And finally imposing the condition $W_0'(0)=0$ as a result of the continuity equation, we generate the ultimate eigenrelation

$$\begin{aligned}iA_1\Delta^{1/2}\tfrac{U_{10}}{T_w}&=iA_1\Delta^{3/4}\omega_0I_1+\tfrac{\gamma_0^2}{T_w}CI_2+i\tfrac{\beta_0}{T_w^3}A_1[1+\tfrac{\bar{v}_0^2}{\bar{u}_0^2}]\bar{u}_0I_3\\ &-6A_1\Delta\tfrac{T_w\bar{T}_0}{U_c(0,0)}I_4+A_1(\sigma-1)\Delta\tfrac{T_w^3\bar{\rho}_0}{U_c(0,0)}I_5.\end{aligned} \tag{3.11}$$

It is easy to notice that the above relation differs from the one obtained before in [31] and [36] for the incompressible flow and in [2] for the compressible flow through the frequency term ω_0 entering in (3.11). Some manipulation of equation (3.11) results in the subsequent eigenrelation for the effective scaled wavenumber γ and scaled wave frequency ω

$$a_2\Omega+b_2\gamma^{1/4}-\gamma^{9/4}=0, \tag{3.12}$$

where the coefficients are presented in [39]. It can be immediately deduced that, whenever (3.12) holds, a neutral stability takes place at the location, say, $r=\bar{r}$.

Having determined the linear terms, we now consider the terms arising from the non-linear interactions in the governing equations in the lower deck. From equating coefficients of like powers of ε from the terms proportional to $\delta^2 E^2$ in (3.4–3.8) and likewise manipulations of the resulting equations together with the zero normal-derivative on the wall will yield the relation

$$\begin{aligned} &C_2\{4\gamma_0^2\tfrac{I_2}{T_w}+\tfrac{i}{T_w^3}\tfrac{\gamma}{\beta_0}U^{0^2}\bar{u}_0 I_3-\tfrac{i}{T_w}\tfrac{\gamma}{\beta_0^2}(2\Delta)^{1/2}U_{10}+i\tfrac{\gamma}{\beta_0^2}\omega_0 I_1(2\Delta)^{3/4}\\ &-6\tfrac{\gamma}{\beta_0^2}\Delta\tfrac{T_w\bar{T}_0}{U_c(0,0)}I_4+\tfrac{\gamma}{\beta_0^2}(\sigma-1)\Delta\tfrac{T_w^3\bar{\rho}_0}{U_c(0,0)}I_5\}=C_1^2\tfrac{\gamma^2}{\beta_0^4}(2\Delta)^{3/2}T_w^2, \end{aligned} \tag{3.13}$$

which associates the amplitude of the first harmonic C_2 to C_1. A similar argument as above leads to the amplitude of the second harmonic C_3, which is related to C_1 through the relation

$$\begin{aligned} &C_3\{9\gamma_0^2\tfrac{I_2}{T_w}+\tfrac{i}{T_w^3}\tfrac{\gamma}{\beta_0}U^{0^2}\bar{u}_0 I_3-2\tfrac{i}{T_w}\tfrac{\gamma}{\beta_0^2}(3\Delta)^{1/2}U_{10}+\tfrac{3i}{2}\tfrac{\gamma}{\beta_0^2}\omega_0 I_1(3\Delta)^{3/4}\\ &-6\tfrac{\gamma}{\beta_0^2}\Delta\tfrac{T_w\bar{T}_0}{U_c(0,0)}I_4+\tfrac{\gamma}{\beta_0^2}(\sigma-1)\Delta\tfrac{T_w^3\bar{\rho}_0}{U_c(0,0)}I_5\}=C_2C_1^*\tfrac{\gamma^2}{\beta_0^4}(3\Delta)^{3/2}T_w^2, \end{aligned} \tag{3.14}$$

in which the last appearing term is owing to the non-linear terms and * denotes complex conjugate. Next, we proceed to the terms proportional to $\delta^3 E$, which are basically very similar to the δE equations in (3.4–3.8). As implemented above, the relation linking the amplitude of the third harmonic C_4 to C_1 is found to be

$$\begin{aligned} &C_4\{-\tfrac{i}{T_w}\tfrac{\gamma}{\beta_0^2}U_{10}+\Delta^{-1/2}[\gamma_0^2\tfrac{I_2}{T_w}+\tfrac{i}{T_w^3}\tfrac{\gamma}{\beta_0}U^{0^2}\bar{u}_0 I_3]+i\tfrac{\gamma}{\beta_0^2}\omega_0 I_1\Delta^{1/4}\\ &-6\tfrac{\gamma}{\beta_0^2}\Delta\tfrac{T_w\bar{T}_0}{U_c(0,0)}I_4+\tfrac{\gamma}{\beta_0^2}(\sigma-1)\Delta\tfrac{T_w^3\bar{\rho}_0}{U_c(0,0)}I_5\}=C_2C_1^*\tfrac{\gamma^2}{\beta_0^4}\Delta T_w^2. \end{aligned} \tag{3.15}$$

And finally, the mean-flow correction terms from the solutions of the δ^2 terms in (3.4–3.8), together with the anticipation of zero-slip on the wall as well as the match with the main deck, are obtained as

$$U_{m0}=r\frac{\gamma}{\beta_0^2}C_2\frac{\bar{u}_1}{T_w^2}\zeta,\quad V_{m0}=r\frac{\gamma}{\beta_0^2}C_2\frac{\bar{v}_1}{T_w^2}\zeta,\quad W_{m0}=-\frac{\gamma}{\beta_0^2}C_2\frac{\bar{u}_1}{T_w^2}\zeta^2. \tag{3.16}$$

4. Results and discussion.

4.1. *Linear results.* Since the linear evolution of the neutral compressible modes was discussed in detail for the zero-suction case in [39] and for suction/blowing applied in [45], we only give a brief outline here. Within this connection, Figure 1 (a-d) shows the scaled leading-order wavenumber against the frequency for a suction $\bar{s}=5$ at the selected Mach numbers 0, 1, 2, and 3, and also for a blowing $\bar{s}=-5$ at the selected Mach numbers 0, 0.5, and 1, respectively, within the domain of definition of local Mach numbers. Asymptotic results corresponding to the large suction or blowing limit as obtained in the Appendix are also shown by the starred curves, which are in excellent agreement with the calculated results. As the Mach number increases towards its cut-off value, the trend is the same as when no-suction is applied as in [39]. However, as the suction parameter is increased, its value for small Mach number is substantially increased. From a linear stability analysis point of view, suction is found to be stabilizing, whereas injection enhances the instability as compared to the no-suction through the surface of the disk, in line with the outcome of [46]. In both cases, positive frequency waves are found to be highly destabilized as compared to the waves having negative frequencies. As also pointed out in [39] and [45], there occurs a double mode region over the positive

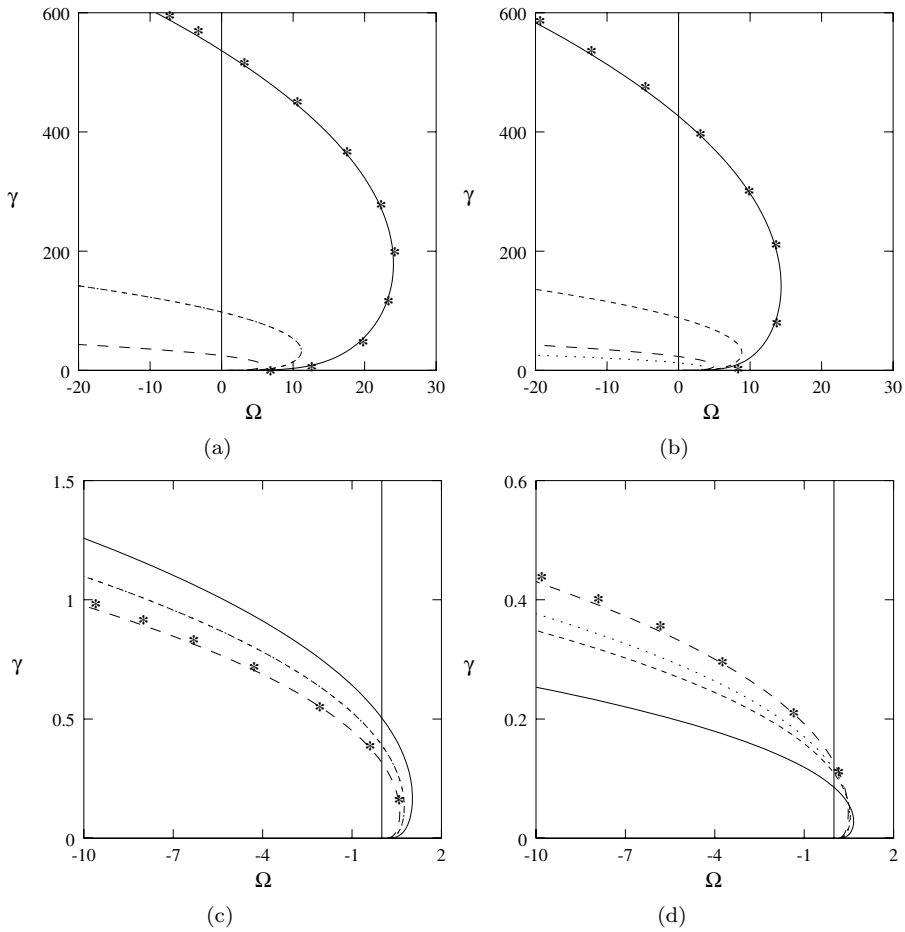

FIG. 1. The development of non-stationary neutral leading-order wavenumber against the frequency are demonstrated for the compressible modes for the suction $\bar{s} = 5$ in (a) $M = 0.0$, in (b) $M = 2$, and for the injection $\bar{s} = -5$ in (c) $M = 0.0$, in (d) $M = 1$, respectively. Curves are for both heat transfer with $T_w = 1.5$ (— —), 1 (– –), and 0.6 (—), and wall insulation (...). Also stars show the asymptotic results of large suction/blowing limits as given in the Appendix.

frequency disturbances. The impact of wall insulation and heat transfer is toward the reduction of the interval of double modes for positive frequencies as the Mach number increases, while the wall cooling rapidly increases the size of the interval for the suction case, with a reverse effect for the injection case. The impacts are more pronounced in the case of wall suction. In addition to this, it can also be seen that although the high-cooling case persists to have larger wavenumbers especially for large suction, the perturbations received into the compressible boundary layer will evolve on a much longer wavelength as the local Mach number attains its highest value in its domain of definition. To conclude from the linear stability point of view, the compressibility destabilizes as

the Mach number increases, making the flow more convectively unstable. However, the non-linearity may totally alter the situation, as will be discussed next.

We remind the reader that the scaled wave angle correction term from the eigenrelation (3.12) was also calculated in [45] together with a comparison to the full linearized stability equations. The boundary layer growth contributes in the way of destabilizing all the modes, in particular for the compressible modes, though the wall cooling in the case of suction and the wall insulation and heating in the case of injection are found to persist to the destabilization for the modes in the vicinity of the stationary mode. Below we proceed to examine the impacts of non-linearity on the stability of the flow.

4.2. *Non-linear results.* [2] and [36] showed that to obtain a classical evolution equation for a non-linear disturbance involving derivatives with respect to r, it is necessary to take account of disturbances of amplitude $O(\varepsilon^{5/2})$ within the lower deck where the non-linearity is first important. This mode then develops in an $O(\varepsilon)$ neighborhood of the neutral position as determined in (3.12) by $r = \bar{r}$. Considering this, as in [2], we perturb the solution from the position of neutral stability by writing

$$r = \bar{r} + \epsilon r_1, \tag{4.1}$$

as a result of which the radial derivative of a quantity is replaced by

$$\frac{\partial}{\partial r} = i\frac{\alpha_0}{\varepsilon^4} + i\frac{\alpha_1}{\varepsilon^2} + \frac{1}{\varepsilon}\frac{\partial}{\partial r_1} + \cdots . \tag{4.2}$$

We additionally replace r from (4.1) in the governing equations (2.1–2.4) and rewrite the expansions of the perturbation quantities (3.4–3.8) in the lower deck. Thus the disturbance velocity $\tilde{U}$ will expand as

$$\begin{aligned}\tilde{U} = \varepsilon^{7/2}\{&[\varepsilon^{-1}\bar{r}A_1(\frac{\bar{u}_0}{T_w} + 2\varepsilon\frac{\bar{u}_1}{T_w^2}\zeta + \cdots) + \varepsilon^{-1}(\bar{U}_{-1} + \varepsilon\bar{U}_0 + \cdots)]E \\ &+\varepsilon^{-1/2}[\bar{r}\frac{A_2}{2}(\frac{\bar{u}_0}{T_w} + 2\varepsilon\frac{\bar{u}_1}{T_w^2}\zeta + \cdots) + (\bar{U}_{20} + \varepsilon\bar{U}_{21} + \cdots)]E^2 + \varepsilon^{1/2}(\bar{U}_{m0} + \varepsilon\bar{U}_{m1} + \cdots) \\ &+ [\bar{r}\frac{A_3}{3}(\frac{\bar{u}_0}{T_w} + 2\varepsilon\frac{\bar{u}_1}{T_w^2}\zeta + \cdots) + (\bar{U}_{30} + \varepsilon\bar{U}_{31} + \cdots)]E^3\} + O(\varepsilon^4) + c.c.,\end{aligned} \tag{4.3}$$

together with a similar expression for $\tilde{V}$, $\tilde{\rho}$, and $\tilde{T}$, while $\tilde{W}$ and $\tilde{P}$ expand as

$$\begin{aligned}\tilde{W} = \varepsilon^{7/2}\{&\{-\varepsilon^5 iA_1[(\alpha_0 r\frac{\bar{u}_1}{T_w^2} + \beta_0\frac{\bar{v}_1}{T_w^2})\zeta^2 + \cdots] + \varepsilon^6(\bar{W}_0 + \varepsilon\bar{W}_1 + \cdots)\}E \\ &+ \varepsilon^{1/2}[-\varepsilon^5 iA_2[(\alpha_0 r\frac{\bar{u}_1}{T_w^2} + \beta_0\frac{\bar{v}_1}{T_w^2})\zeta^2 + \cdots] + \varepsilon^6(\bar{W}_{20} + \varepsilon\bar{W}_{21} + \cdots)]E^2 \\ &+ \varepsilon^{19/2}(\bar{W}_{m0} + \varepsilon\bar{W}_{m1} + \cdots) \\ &+ \{-\varepsilon^6 iA_3[(\alpha_0 r\frac{\bar{u}_1}{T_w^2} + \beta_0\frac{\bar{v}_1}{T_w^2})\zeta^2 + \cdots] + \varepsilon^7(\bar{W}_{30} + \varepsilon\bar{W}_{31} + \cdots)\}E^3\} + O(\varepsilon^{10}) + c.c.,\end{aligned} \tag{4.4}$$

$$\begin{aligned}\tilde{P} = \varepsilon^{7/2}\{&\varepsilon^3(\bar{P}_0 + \varepsilon P_1 + \cdots)E + \varepsilon^{5/2}(\bar{P}_{20} + \varepsilon\bar{P}_{21} + \cdots)E^2 \\ &+ \varepsilon^{27/2}(\bar{P}_{m0} + \varepsilon\bar{P}_{m1} + \cdots) + \varepsilon^4(\bar{P}_{30} + \varepsilon\bar{P}_{31} + \cdots)E^3\} + O(\varepsilon^8) + c.c.,\end{aligned} \tag{4.5}$$

where now quantities depend upon r_1 and ζ. The aim of the weakly non-linear analysis is to determine $C_1(r_1)$. In order to obtain the required eigenrelation involving terms proportional to C_1, r_1C_1, $\frac{dC_1}{dr_1}$, and $C_1|C_1|^2$, equations (4.3–4.5) are substituted into the

non-linear disturbance equations obtained by perturbing (2.1–2.4), and coefficients of like powers of ε in the terms proportional to E are equated to solve for $\bar{W}_1$. Following the analysis of [2], the solution to $\bar{W}_1$ is obtained as

$$\begin{aligned}
&\bar{W}_1 = -i\beta_2\tfrac{\bar{v}_0}{T_w}\Delta^{-1/4}A_1 s - \bar{r}\tfrac{\bar{u}_0}{T_w}\Delta^{-1/4}s\tfrac{dA_1}{dr_1} + \tfrac{i}{\bar{r}}\beta_1\tfrac{\bar{v}_0}{T_w}\Delta^{-1/4}r_1A_1 s \\
&+\tfrac{i}{\bar{r}}r_1\tfrac{U_{10}}{T_w}\Delta^{-1/4}A_1 s\tfrac{\beta_0^2M_\infty^2}{\gamma^2} - \tfrac{i}{\bar{r}}\omega_0F_1(s)r_1A_1(1+\tfrac{\beta_0^2M_\infty^2}{\gamma^2}) + \Delta^{-3/4}\{-\tfrac{2}{\bar{r}}r_1C_1\gamma_0^2\tfrac{F_2(s)}{T_w} \\
&-2\tfrac{i}{\bar{r}}\beta_0{U^0}^2\bar{u}_0r_1A_1\tfrac{F_3(s)}{T_w^3U_c(0,0)}(1+\tfrac{\beta_0^2M_\infty^2}{\gamma^2}) - 6\tfrac{r_1}{\bar{r}}T_w\Delta A_1\tfrac{F_4(s)}{U_c(0,0)}[-\bar{T}_0(1+\tfrac{\beta_0^2M_\infty^2}{\gamma^2}) + 2bT_w^2] \\
&+\tfrac{r_1}{\bar{r}}T_w^3\Delta(\sigma-1)A_1\tfrac{F_5(s)}{U_c(0,0)}[-\bar{\rho}_0(1+\tfrac{\beta_0^2M_\infty^2}{\gamma^2}) - 2b]\} - \Delta^{3/4}T_w^2A_2A_1^*s \\
&-k_1\tfrac{r_1}{\bar{r}}\zeta^2 + O(\zeta^2) + A_1RHS,
\end{aligned} \tag{4.6}$$

where $b = (\Gamma-1)M^2f_1'(0)/(4T_w^3)$ and the RHS term contains various eigenvalues as well as perturbation quantities (including also terms proportional to the suction parameter $\bar{s}$), whose precise shape will turn out to be unimportant for the subsequent analysis. Moreover, the satisfaction of the boundary conditions on the wall in the continuity equation gives the solvability condition

$$\frac{\partial\bar{W}_1}{\partial s} - i\frac{r_1}{\bar{r}^3}U_{10}\Delta^{-1/4}A_1\frac{\beta_0^2M^2}{\gamma^2} - \frac{\bar{s}}{R_w}\frac{\partial\bar{\rho}_0}{\partial s} = 0 \quad \text{at} \quad s = 0. \tag{4.7}$$

Furthermore, as a consequence of the use of (4.7) together with (4.6) we obtain the following amplitude equation on C_1:

$$\begin{aligned}
&\tfrac{dC_1}{dr_1} = r_1C_1\{i\tfrac{\beta_1\bar{v}_0}{\bar{r}^2\bar{u}_0} + \tfrac{\beta_0^4\gamma_0^2M^2I_2}{\bar{r}^4\Delta^{1/2}\bar{u}_0\gamma^3} - \tfrac{\beta_0^2\gamma_0^2I_2}{\bar{r}^2\Delta^{1/2}\bar{u}_0\gamma} - i\tfrac{U_{10}}{\bar{r}^2\bar{u}_0}(1+\tfrac{\beta_0^2M^2}{\bar{r}^2\gamma^2}) \\
&-\tfrac{12bTw^4\Delta^{1/2}I_4}{\bar{r}^2\bar{u}_0U_c(0,0)} - \tfrac{2bT_w^4(\sigma-1)\Delta^{1/2}I_5}{\bar{r}^2\bar{u}_0U_c(0,0)}\} - \tfrac{C_1^*C_2\gamma T_w^3\Delta}{\bar{r}\beta_0^2\bar{u}_0} + \tfrac{\Delta^{1/4}T_w}{\bar{r}\bar{u}_0}I_6C_1 = 0,
\end{aligned} \tag{4.8}$$

for which I_6 is given by a complex contour integration as

$$I_6 = \frac{1}{2U_c(0,0)}\int_0^\infty \theta U_c(0,\theta)RHS(\sqrt{2}s = \theta)d\theta, \tag{4.9}$$

and the correspondence of C_2 can be obtained from (3.13) as

$$\begin{aligned}
&C_2 = C_1^2 2\sqrt{2}\Delta^{3/2}T_w^2\gamma_0M_1^2\{4\gamma_0\beta_0^4\tfrac{I_2}{T_w} + i\tfrac{{U^0}^2\bar{u}_0I_3M_1\beta_0^3}{T_w^3} - i\sqrt{2}\beta_0^3\Delta^{1/2}\bar{r}\bar{u}_0M_1\tfrac{\Phi_0}{T_w} \\
&-\tfrac{6T_w\bar{T}_0\Delta\beta_0^2M_1I_4}{U_c(0,0)} + \tfrac{T_w^3(\sigma-1)\bar{\rho}_0\Delta\beta_0^2M_1I_5}{U_c(0,0)} + i\omega_0I_1\beta_0^2 2^{3/4}\Delta^{3/4}M_1\}^{-1},
\end{aligned} \tag{4.10}$$

where $M_1 = \sqrt{1-\frac{M^2}{{U^0}^2}}$ and $\Phi_0 = [\frac{\alpha_1}{\beta_0} - \frac{\beta_1\alpha_0}{\beta_0^2}]$.

Next, we rewrite equation (4.8) in the form

$$\frac{dC_1}{dr_1} = (a+ib_1)r_1C_1 + (c+id)C_1|C_1|^2 + (e+if)C_1, \tag{4.11}$$

where the coefficients a, b_1, c, d, e, and f in (4.11) are real constants. Multiplying (4.11) by the complex conjugate of C_1, adding the complex conjugate and replacing r_1 by $r_2 = r_1 + e/a$ for $a \neq 0$ gives

$$\frac{d|C_1|^2}{dr_2} = 2c|C_1|^4 + 2ar_2|C_1|^2. \tag{4.12}$$

It is true that the amplitude equation does not involve the suction parameter $\bar{s}$ explicitly. However, the imposition of suction or blowing directly affects the non-linear evolution of a disturbance, since an implicit dependence of the coefficients in (4.12) on the suction parameter through the basic flow quantities is apparent. Moreover, the amplitude equation

we obtained in (4.12) is in the same form as the one in [2] and [1], but the coefficients now depend on the frequency term ω_0. Indeed, the scaled parameter c is given by using (4.8) and (4.10) as $c = B\bar{r}^{-13/4}$, where B is expressed by

$$B = \frac{1}{2\sqrt{2}}|\frac{\bar{v}_0}{u_0}|^{5/2}\frac{U^{0^{3/2}}}{\bar{u}_0}\frac{M_1^3}{T_w^5}\gamma^{1/2}\frac{(\kappa_1-\kappa_2)}{(\kappa_1^2+\kappa_2^2)}, \tag{4.13}$$

in which $\kappa_1 = (4-\sqrt{2})\gamma^3 U^{0^{-2}} I_2/T_w + [1-2^{-1/4}]\cos(\pi/8)M_1|\frac{\bar{v}_0}{U^0\bar{u}_0}|^{3/4}\Omega I_1\gamma^{3/4}/T_w^3$ and $\kappa_2 = (1-\sqrt{2})\gamma^3 U^{0^{-2}} I_2/T_w + [(2^{-3/4}-2^{-1/4})\cos(\pi/8) + (1-2^{-3/4})\sin(\pi/8)]$ $M_1|\frac{\bar{v}_0}{U^0\bar{u}_0}|^{3/4}\Omega I_1\gamma^{3/4}/T_w^3$.

The effects of suction and blowing on the value of the parameter B defined in (4.13) are demonstrated for a large suction $\bar{s} = 5$ in Figure 2 (a-b) and for a large blowing $\bar{s} = -5$ in Figure 2 (c-d) for both adiabatic and insulated wall conditions. It is found that the behavior of stationary compressible modes and non-stationary incompressible modes is in total agreement with those of [2] and [45], respectively. In spite of the fact that Figure 2 (a-d) represents specific cases of a suction and injection (and restricted Mach numbers), the general trend for values of $\bar{s} > 0$ and $\bar{s} < 0$ is similar to those in Figure 2 (a-d). The trends calculated for zero-suction incompressible modes in [40] are preserved here for large blowing, while an opposite behavior is seen for the large suctioning, in particular for an isothermal wall as the Mach number increases. An immediate conclusion to be drawn from Figure 2 (a-d) is that the non-linear effects are destabilizing for a linearly unstable disturbance for all of the Mach numbers within which the neutral stationary or non-stationary waves exist, since B is positive for both suction and injection. In addition to this, the values of B for the suction case are much larger than those of injection, thus the nonlinear effects are stronger for a mode under the influence of strong suction. Moreover, although a mode with high cooling applied is more destabilizing for the suction case, a mode created as a result of an adiabatic wall or an isothermal wall with $T_w \geq 1$ has the same effect for the blowing case. Furthermore, another significant finding is that compressibility as the Mach number increases is seen to have a destabilizing impact for suctioning for particular modes in the vicinity of the stationary mode, whereas a reverse effect is observed for blowing for all the modes. The final outcome that can be deduced from Figure 2 (a-d) is that no matter whether adiabatic or isothermal wall and suction or blowing on the wall are considered, B is greater for the disturbances having positive frequencies as compared to those having negative frequencies. Therefore, for such modes the destabilizing effects of non-linearity will be much larger for a compressible flow with non-stationary positive frequencies than for an incompressible flow of [12] or for a compressible flow of [1] having the stationary modes.

The second coefficient of (4.12), a is also given by using (4.8) and (4.10) as $a = A\bar{r}^{-7/4}$, where A is expressed by

$$A = -\frac{\gamma^{5/2}U^{0^{-3/2}}T_w^2 I_2}{M_1^3|u_0v_0|^{1/2}} + \frac{bT_w^2\gamma^{1/2}U^{0^{-1/2}}|v_0|^{1/2}}{|u_0|^{3/2}U_c(0,0)}[-6I_4 - (\sigma-1)I_5]. \tag{4.14}$$

The ultimate state of the disturbed flow field can be determined by the values of A, the behavior of which is demonstrated next in Figure 3 (a-b) for the large suction case and in Figure 3 (c-d) for the large blowing case taking into account both adiabatic and

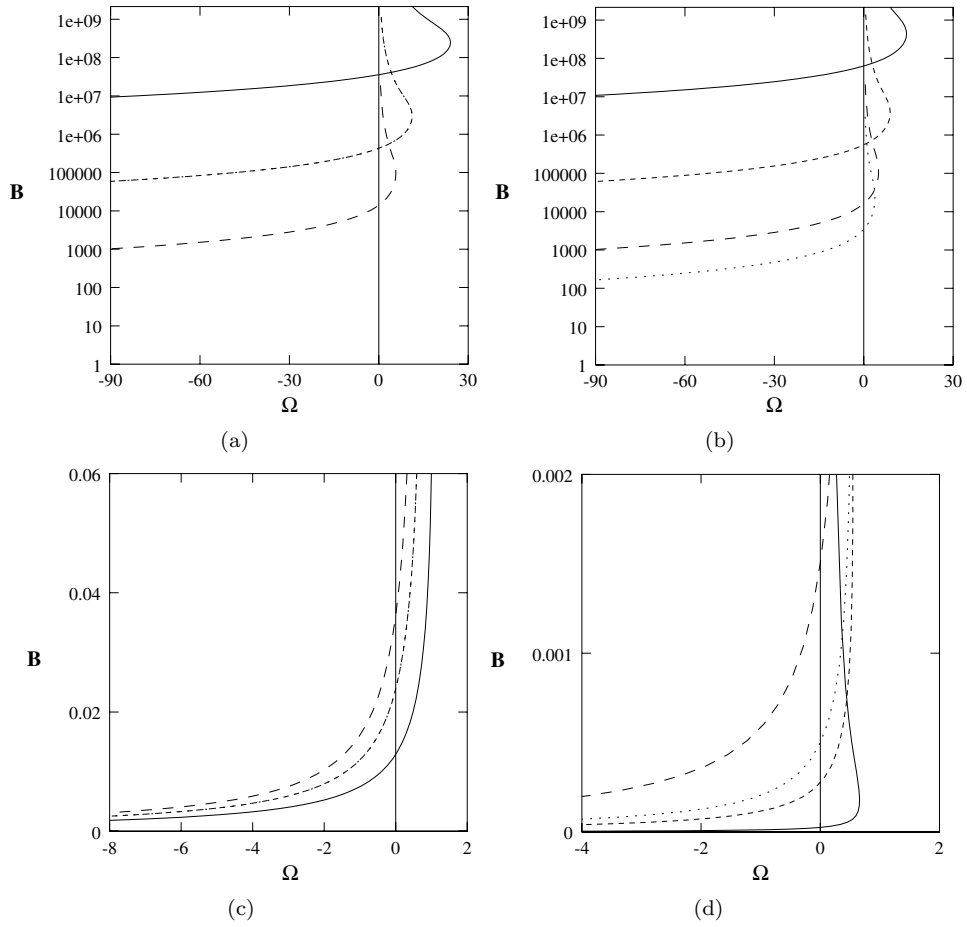

FIG. 2. The development of the parameter B is displayed as a function of Ω for an adiabatic wall (...) and for an isothermal wall with $T_w = 1.5$ (— —), 1 (– –), and 0.6 (—) at the chosen Mach numbers, for the suction $\bar{s} = 5$ (a) $M = 0$, (b) $M = 2$ and for the injection $\bar{s} = -5$ (c) $M = 0$ and (d) $M = 1$.

isothermal wall conditions. Again the graphs are fully consistent with those displayed in [1] in the case of stationary compressible modes. Although the trend in the case of large suction is similar to zero-suction non-stationary compressible modes, it differs in the case of large blowing. The effect of compressibility is seen to increase the value of A for large suction, particularly in the case of high cooling, whereas it decreases A substantially in the case of large blowing for all of the modes. Regardless of the wall insulation or heat transfer through the wall or suction (for small Mach numbers) and blowing, a region of disturbances with positive frequencies also having positive A is observed, corresponding to the lower part of the double modes as shown in Figure 1 (a-d). Additionally, the upper part of the double modes also has positive value of A as the Mach number increases. Moreover, as compressibility is stronger, not only the

positive frequency waves but also the negative frequency waves receive positive value of A. Although not shown here, such modes extend onto $\Omega = -62$ for $\bar{s} = 5$ with $M = 3$ and $T_w = 0.6$. The importance of such modes with positive value of A is that for these modes the amplitude of the disturbance increases continuously as the distance from the neutral radius is increased; that is, the solution will be always unstable. Thus, for large suction the range of local Mach number over which a stable solution can exist decreases in the case of heat transfer with T_w small. However, whenever the sign of A is negative as shown in Figure 3 (a-d), an unstable solution can only occur if a disturbance is away from the neutral location, otherwise the amplitude of the disturbance decreases.

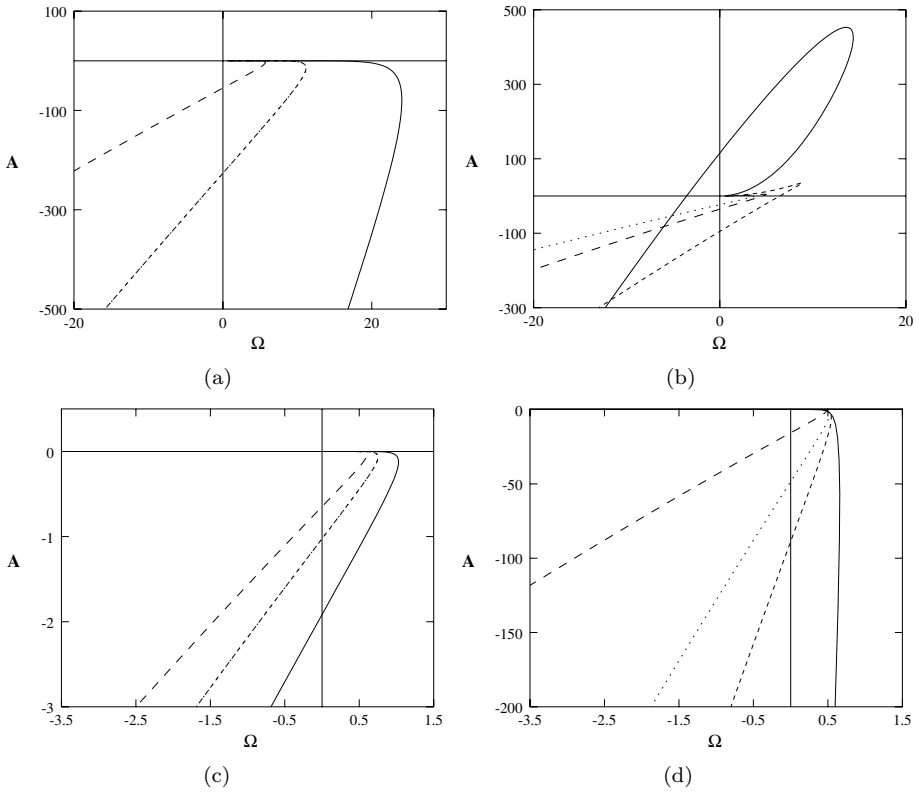

FIG. 3. The development of the parameter A is displayed as a function of Ω for an adiabatic wall (...) and for an isothermal wall with $T_w = 1.5$ (— —), 1 (– –), and 0.6 (—) at the chosen Mach numbers, for the suction $\bar{s} = 5$ (a) $M = 0$, (b) $M = 2$ and for the injection $\bar{s} = -5$ (c) $M = 0$ and (d) $M = 1$.

Applying the same transformations to the amplitude equation (4.12) as in [2], we reach the solution for the amplitude function of any given disturbance as

$$|C_1| = \begin{cases} \sqrt{\frac{\sqrt{a}}{2c}} \frac{e^{x^2/2}}{(y_0^{-1} - \int_0^x e^{t^2} dt)^{1/2}}, & a > 0, \\ \sqrt{\frac{e}{c}} \frac{e^{x/2}}{(y_0^{-1} + 1 - e^x)^{1/2}}, & a = 0, \\ \sqrt{\frac{\sqrt{|a|}}{2c}} \frac{e^{-x^2/2}}{(y_0^{-1} - \int_0^x e^{-t^2} dt)^{1/2}}, & a < 0, \end{cases} \tag{4.15}$$

where $y_0 = y(0)$, $x = 0$ corresponds to the neutral position and x is given by

$$x = \begin{cases} \sqrt{|a|} r_2, & a \neq 0, \\ 2e r_1, & a = 0. \end{cases} \tag{4.16}$$

The result (4.15) is a generalization of the stationary and non-stationary non-linear disturbance amplitude, which is valid for both incompressible and compressible flows under either the influence of suction or injection through the surface of the disk, i.e., the cases that were previously investigated by several authors, such as [36], [2], [12], [1], and [40, 45]. It can be easily seen from equation (4.15) that for $a \geq 0$ (see also Figure 3 (a-d)), the solutions will grow unboundedly and terminate at a finite value of the radius, leading to an unstable solution. However, for $a < 0$ the same results hold for the non-stationary compressible problem as for the stationary compressible problem of [1]. Therefore, as described in these works, a critical value exists for the initial amplitude of the disturbance above which the disturbance will amplify infinitely at a specific radius, leading to an unstable solution and below which the disturbance will grow initially but will eventually decay to zero, leading to a stable solution. In line with the previous research, this critical value is found to be $y_0 = 2/\sqrt{\pi}$ for both suction and blowing. For $a < 0$ then the scaled threshold amplitude can be given by

$$T = \bar{r}^{-19/8} |C_1|^2|_{x=0} y_0^{-1} = \sqrt{\frac{-A}{4B^2}}. \tag{4.17}$$

To be able to understand whether suction or blowing makes a mode crucial and also to compare the likelihood of appearance of modes of compressible or incompressible kind, we plot the threshold amplitude T, defined in (4.17), of the perturbations in Figures 4 (a-d) and 5 (a-c). In the case of large suction, Figure 4 (a-d) demonstrates that the threshold amplitude for highly cooled walls is much smaller, as compared to the values for a range of the local Mach numbers, than for an adiabatic wall or for an isothermal wall. What is more intriguing here is that the modes corresponding to the high cooling case (which are missing in Figures 4 and 5 but instead shown in Figure 3 (a-b)) are already unstable regardless of the initial amplitude not only for positive frequencies but also for negative frequencies. This property extends to cover isothermal wall modes too, for sufficiently large Mach numbers. In addition to this, as the local Mach number increases, the value of the initial amplitude of the disturbance required to cause an unstable solution decreases, except for the modes born particularly from the adiabatic wall conditions for which compressibility has a stabilizing effect. On the other hand, compressibility as the Mach number increases has a destabilizing effect when the isothermal wall is considered, a result just opposite to the modes of [2]. Moreover, this finding completely contradicts

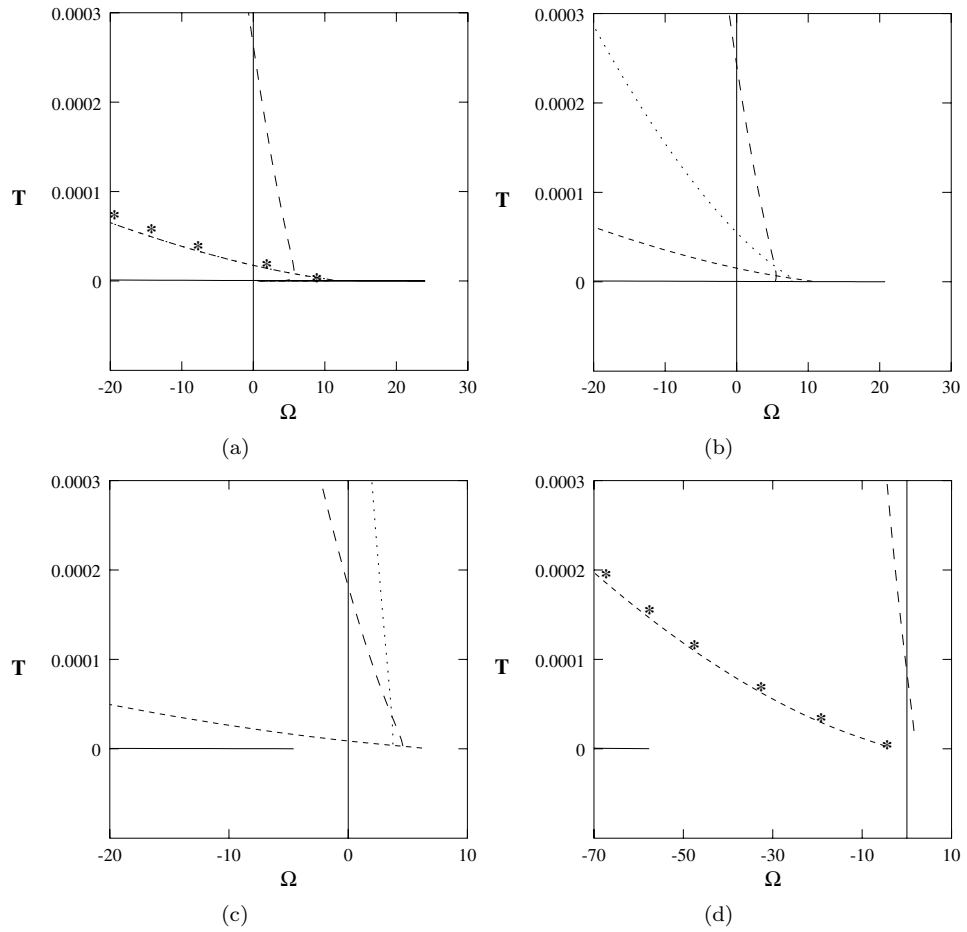

FIG. 4. The development of the initial amplitude disturbance parameter T for the suction $\bar{s} = 5$ is displayed as a function of Ω for an adiabatic wall (...) and for an isothermal wall with $T_w = 1.5$ (— —), 1 (– –), and 0.6 (—) at the chosen Mach numbers (a) $M = 0$, (b) $M = 1$, (c) $M = 2$, and (d) $M = 3$. Also, stars show the asymptotic results of large suction/blowing limits as given in the Appendix.

the findings of linear modes in Section 4.1 in that compressibility when the adiabatic wall condition is considered is destabilizing, but for isothermal walls in particular for high cooling it is stabilizing.

As for the large blowing case, Figure 5 (a-c) shows that much larger initial amplitude is required in this case as compared to the large suction case, indicating the stabilizing influence of fluid injection for the non-linear disturbances. Moreover, larger Mach numbers lead to enhanced values of the threshold parameter, and thus the compressibility is also stabilizing. However, in contrast to the zero-suction findings of [2], the imposition of blowing increases the threshold amplitude for highly cooled walls for both stationary and some non-stationary modes as compared to the adiabatic wall or heat transfer cases

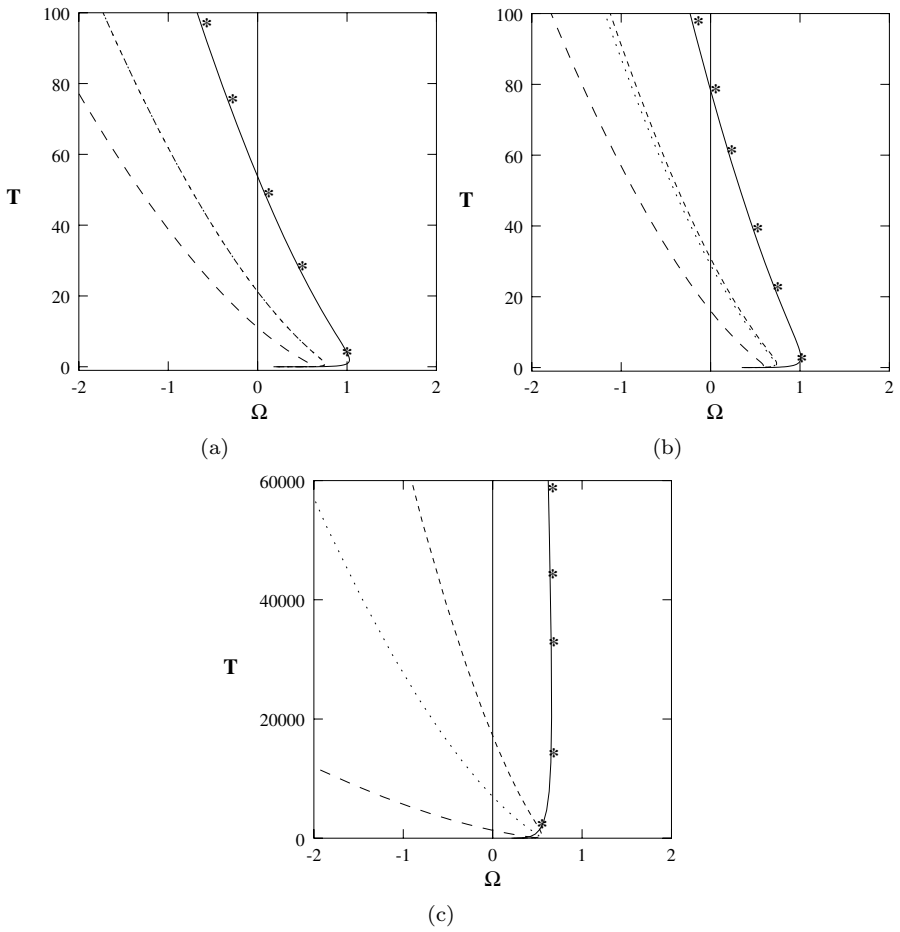

FIG. 5. The development of the initial amplitude disturbance parameter T for the injection $\bar{s} = -5$ is displayed as a function of Ω for an adiabatic wall (...) and for an isothermal wall with $T_w = 1.5$ (— —), 1 (– –), and 0.6 (—) at the chosen Mach numbers (a) $M = 0$, (b) $M = 0.5$, and (c) $M = 1$. Also, stars show the asymptotic results of large suction/blowing limits as given in the Appendix.

with $T_w > 1$, thus decreasing the possibility of occurrence of such modes in an unstable state.

Figures 4–5 also show the asymptotic results (starred curves) as computed from the large suction/injection limits obtained in the Appendix. The asymptotic results are in excellent agreement with the threshold amplitudes as calculated from (4.17). It is also apparent for both suction and blowing from Figures 4 (a-d) and 5 (a-c) that in parallel to the previous findings, perturbations having positive frequencies will amplify prior to the other disturbances including the compressible stationary modes of [2] to carry the flow into an unstable state. Whether suction or blowing is applied to the disk, highly cooled modes are likely to be more dangerous than the adiabatic or heat

transfer cases. These outcomes can also be justified by examining the asymptotic large suction/blowing behavior of the quantities given in the Appendix. It is seen in the Appendix that for positive frequencies with the scaled wavenumber γ small, the initial amplitude $|C_1||_{x=0}$ will be on the order of magnitude of $\gamma^{7/4}$ for an adiabatic wall and of $\gamma^{3/4}$ for an isothermal wall, whereas for negative frequencies with γ large, it will be on the order of magnitude $\gamma^{15/4}$. This implies that for the total amplification of the perturbations received into the three dimensional rotating-disk boundary layer, a smaller amplitude will be sufficient for the positive frequency waves (generated as a result of highly cooled walls) than for the negative ones. Thus, the destabilizing influences of non-linearity are greater for a positive frequency disturbance than for a negative one, resulting in the fact that for the negative frequencies close to the neutral location the non-linear effects are less important. This enables us to conclude that transition from laminar flow to turbulence may first take place through the amplification of the disturbances having positive frequencies rather than through the zero-frequency modes of [2], if of course the lower branch modes calculated here dominate over the inviscid upper branch modes of [14]. If this is the case, then the non-stationary short-wavelength unstable modes described in this paper could be observed experimentally as in [23] and [37, 38].

5. Conclusions. The triple-deck theory has been implemented in this work to investigate theoretically the linear and non-linear evolution of stationary and non-stationary short-wavelength small frequency lower branch modes of the disturbances imposed on the basic compressible three-dimensional boundary layer flow induced by a rotating disk. Particular interest has been taken to search for the possible influences of suction and blowing applied to the disk on the modes especially developing non-linearly. The imposition of suction or blowing on the three-dimensional compressible boundary layer has been shown to have a significant effect on the mean flow, which in turn influences the stability properties of this boundary layer. The effects of non-parallelism were determined in detail previously in [45] on the evolution of compressible linear lower branch modes, which has also been briefly reviewed here for comparison purposes. In place of the linear evolution, we rather concentrate here on the influences of the non-linearity on the time-dependent solutions, but quite close to the linear stationary neutral waves having vanishingly small shear stress on the wall. On this ground, an amplitude equation has been extracted and, as a result of solving this equation, disturbances that grow or decay with respect to the positions from the location of neutral stability have been determined for both suction and injection. To summarize, for both suction and blowing, the non-linearity always has a destabilizing impact on the three-dimensional rotating-disk boundary layer flow. The destabilization influence of the non-linearity is particularly pronounced for the positive short-wavelength frequency waves; however, negative frequency waves with highly cooled walls are also destabilized for large suction limit. Also, even though the modes as a result of adiabatic wall conditions are found to be stabilized in the case of suction as the local Mach number increases, modes with high cooling conditions are stabilized in the case of injection. The asymptotic large suction/blowing limits have been shown to excellently agree with the numerical results.

The compressibility has different influences on the evolution of linear and non-linear lower branch modes. As far as the linear modes are concerned, suction is highly stabilizing, whereas injection is destabilizing as also concluded in [45]. In addition to this, modes as a consequence of high cooling are the most unstable as the compressibility increases in the case of suction, though an opposite effect is observed in the case of injection for the same modes. However, non-linearity has a strong impact; thus a completely reverse effect has been observed here for the evolution of the non-linear modes.

It has been known since the pioneering works of [36] and [2] that the non-linear influences are more important in lower branch modes close to the neutral locations than in inviscid upper branch modes. Indeed, the trends in the behaviors of the coefficients in the evolution equation clearly show that the non-linearity is destabilizing for the stationary as well as the non-stationary modes existing in the domain of the local Mach number for both suction and injection. Also, the non-linear effects resulting from suction on the surface of the disk are found to be much stronger as compared to the injection. Moreover, in spite of the fact that a mode with high cooling is largely destabilized in the case of suction, it is highly stabilized in the case of injection. In line with the stationary modes of [2], [1], and [12], a threshold amplitude of the perturbations has been demonstrated to exist at the position of neutral stability of the lower branch modes. If at the position of neutral stability, the amplitude of any disturbance is larger than this specific value, the solutions are most likely to grow in size driving the flow into turbulence, as the distance from the neutral stability location is increased. Different from the works of [2], [1], and [12], it has been shown here that in the case of large suction some stationary as well as non-stationary modes are always unstable regardless of the initial amplitude, the extent of which increases as the local Mach number gets bigger. Particularly the modes under the influence of strong suction with cooled walls are subjected to a powerful non-linear instability as the Mach number increases for both the positive and negative frequency waves. On the other hand, not the modes with high cooling but those with large heating are more likely to occur for a blowing, as they attain a smaller threshold amplitude. Compressibility has a stabilizing effect whenever blowing is applied to the disk, whereas it destabilizes the modes generated particularly through the isothermal wall condition. Furthermore, it has been found that the initial amplitude of the modes leading to an infinite growth is much larger for the negative frequency waves as compared to the positive ones, regardless of the suction or injection applied on the flow. Thus, in compliance with the experiments of [37, 38], non-stationary waves having positive or negative (in the case of suction) frequencies with sufficiently small amplitude near the neutral location are of significance in application. These unstable modes are most probably the ones also observed in the experiment of [23]. If, however, the amplitude of a disturbance is smaller than the threshold amplitude, it eventually decays to zero after an initial growth as the distance from the position of neutral stability is increased, leaving the flow stable. In this case, of course, the unstable inviscid mode observed to be dominant in the experiment of [14] will definitely be in action.

To conclude, our results show that an unstable mode of instability is more likely to occur for a compressible flow either due to the existence of positive or negative frequency waves with high cooling in the case of suction or positive frequency waves with heating

or adiabatic wall in the case of injection. In addition to this, suction is absolutely more effective as compared to the blowing. Thus, in the absence of other more dangerous instability mechanisms, the early breakdown of the laminar flow over a rotating disk will be a consequence of the non-linear amplification of the lower branch modes identified in this work.

6. Appendix.

6.1. *The large suction limit.* In this section of the Appendix we give the large suction ($\bar{s} >> 1$) limit behaviors of various quantities for γ fixed and small, particularly the threshold amplitude (2.4) as described in Section 4. Based on the large suction behavior of the wall, derivatives of the velocities given by

$$\bar{u}_0 = \frac{T_w}{2\bar{s}}, \quad \bar{v}_0 = -\frac{\bar{s}}{T_w}, \tag{6.1}$$

the leading-order behavior of the expressions Ω, A, and B in the text can be computed asymptotically:

$$\Omega \sim \frac{B_2 \gamma^{1/4} \bar{s}}{T_w^2 A_2}, \tag{6.2}$$

$$A \sim -\frac{\gamma^{5/2} I_2 T_w^5 \bar{s}^{-3}}{2} - \frac{2 b_0 \gamma^{1/2} \bar{s}^2}{U_c(0,0) T_w^3}[6I_4 + (\sigma - 1) I_5], \tag{6.3}$$

$$B \sim \frac{2^{7/2} A_2^2 \psi_2 \gamma^{-1/2} \bar{s}^8}{B_2 Z I_1^2 T_w^9}, \tag{6.4}$$

where $A_2 = [\cos(\frac{\pi}{8}) - \sin(\frac{\pi}{8})] 2^{-3/4} I_1$, $Z = (\psi_4 \cos(\frac{\pi}{8}))^2 + 2^{-3/2}(\psi_5 \cos(\frac{\pi}{8}) + \psi_2 \sin(\frac{\pi}{8}))^2$, $\psi_2 = 2^{3/4} - 1$, $\psi_4 = 1 - 2^{-1/4}$, and $\psi_5 = 1 - \sqrt{2}$. Additionally, b_0 and B_2 vary in accordance with the consideration of adiabatic or isothermal wall conditions and are thus given by

$$b_0 = \begin{cases} 0, & \text{for an adiabatic wall,} \\ \frac{(\Gamma-1)\sigma M^2}{2}, & \text{for an isothermal wall,} \end{cases}$$

$$B_2 = \begin{cases} I_3 T_w, & \text{for an adiabatic wall,} \\ I_3 T_w + \frac{[6I_4 + (\sigma-1)I_5]}{2U_c(0,0)} \{ \frac{(\Gamma-1)\sigma M^2}{2} + (1 - T_w)\sigma \}, & \text{for an isothermal wall.} \end{cases}$$

Thus the asymptotic behavior of the threshold amplitude is given by

$$T = \frac{\sqrt{-A}}{2B}, \tag{6.5}$$

where the corresponding parameters are given in equations (6.3–6.4).

6.2. *The large blowing limit.* In this section of the Appendix we give the large blowing ($\bar{s} << -1$) limit behaviors of various quantities for γ fixed and large, particularly the threshold amplitude as described in Section 4. Based on the large blowing behavior of the wall derivatives of the velocities given by

$$\bar{u}_0 = -\frac{T_w}{\bar{s}}, \quad \bar{v}_0 = 2\frac{T_w^3}{\bar{s}^3}, \tag{6.6}$$

the leading-order behavior of the expressions Ω, A, and B in the text can be computed asymptotically:

$$\Omega \sim \frac{-\gamma^{9/4} I_2 T_w^2 (-\bar{s})^{3/2}}{A_3}, \tag{6.7}$$

$$A \sim -\frac{\gamma^{5/2} I_2 \bar{s}^2}{\sqrt{2} M_1^3}, \tag{6.8}$$

$$B \sim \frac{2 M_1^3 \psi_9 \gamma^{-5/2} \bar{s}^{-4}}{T_w \psi_8}, \tag{6.9}$$

where $M_1 = (1 - M^2)^{1/2}$, $A_3 = A_2 2^{3/4} M_1 T_w^{3/2}$, $\psi_8 = \psi_6^2 + \psi_7^2$, $\psi_6 = [\psi_3 - \frac{\psi_4}{A_3} 2^{3/4} \cos(\frac{\pi}{8}) M_1 T_w^{3/2} I_1] I_2 / T_w$, $\psi_7 = [\psi_5 - \frac{(\psi_5 \cos(\frac{\pi}{8}) + \psi_2 \sin(\frac{\pi}{8}))}{A_3} 2^{3/4} M_1 T_w^{3/2} I_1] I_2 / T_w$, $\psi_9 = \psi_6 - \psi_7$, and $\psi_3 = 4 - \sqrt{2}$.

Thus the asymptotic behavior of the threshold amplitude is given by

$$T = \frac{\sqrt{-A}}{2B} \sim \frac{T_w I_2^{1/2} \psi_8 \gamma^{15/4} (-\bar{s})^5}{2^{9/4} \psi_9 M_1^{9/2}}. \tag{6.10}$$

It should be remarked that to the leading-order, T in (6.10) gives amplitude of the modes resulting from both the adiabatic as well as the isothermal wall conditions.

References

[1] S. O. Seddougui and A. P. Bassom, *The effects of suction on the non-linear stability of a three-dimensional compressible boundary layer*, IMA Journal of Applied Mathematics, **56** (1996), 183. MR1401182 (97e:76075)

[2] S. O. Seddougui, *A nonlinear investigation of the stationary mode of instability of the three dimensional compressible boundary layer due to rotating-disk*, Q. J. Mech. Appl. Math., **43** (1990), 467–497. MR1081299 (91j:76055)

[3] R. J. Lingwood, *Absolute instability of the boundary layer on a rotating-disk*, J. Fluid Mech., **299** (1995), 17–33. MR1351381 (96e:76061)

[4] J. W. Cole, *Hydrodynamic stability of compressible flows*, PhD Thesis (1995), University of Exeter.

[5] R. J. Lingwood, *An experimental study of absolute instability of the rotating-disk boundary layer flow*, J. Fluid Mech., **314** (1996), 373–405. MR1372076

[6] R. J. Lingwood, *On the application of the Briggs' and steepest-descent method to a boundary layer flow*, Stud. Appl. Maths., **98** (1997), 213–254. MR1441304 (97k:76034)

[7] M. Turkyilmazoglu, *Linear absolute and convective instabilities of some two- and three dimensional flows*, PhD Thesis (1998), University of Manchester.

[8] M. Turkyilmazoglu, J. W. Cole and J. S. B. Gajjar, *Absolute and convective instabilities in the compressible boundary layer on a rotating disk*, Theoret. Comput. Fluid Dyn., **14** (2000), 21–37.

[9] M. Turkyilmazoglu and J. S. B. Gajjar, *Direct spatial resonance in the laminar boundary layer due to a rotating-disk*, SADHANA-ACAD P ENG S., **25** (2000), 601–617.

[10] M. Turkyilmazoglu and J. S. B. Gajjar, *An analytic approach for calculating absolutely unstable inviscid modes of the boundary layer on a rotating-disk*, Stud. Appl. Maths., **106** (2001), 419–435. MR1825844 (2002a:76168)

[11] A. J. Cooper and P. W. Carpenter, *The stability of rotating-disk boundary layer flow over a compliant wall. Part II. Absolute instability*, J. Fluid Mech., **350** (1997), 261–270. MR1481902 (98k:76056)

[12] A. P. Bassom and S. O. Seddougui, *The effects of suction on the nonlinear stability of the three-dimensional boundary layer above a rotating disc*, Proc. Roy. Soc. London Ser. A, **436** (1992), 405–415. MR1177136 (93e:76032)

[13] R. J. Lingwood, *On the effects of suction and injection on the absolute instability of the rotating-disk boundary layer*, Phys. Fluids, **9** (1997), 1317-1328.

[14] N. Gregory, J. T. Stuart and W. S. Walker, *On the stability of three dimensional boundary layers with applications to the flow due to a rotating-disk*, Philos. Trans. R. Soc. London Ser. A, **248** (1955), 155–199. MR0072616 (17:311c)
[15] M. R. Malik, S. P. Wilkinson and S. A. Orszag, *Instability and transition in rotating-disk flow*, AIAA Journal, **19** (1981), 1131–1138.
[16] M. R. Malik, D. I. A. Poll, *Effect of curvature on three dimensional boundary layer stability*, AIAA Journal, **23** (1985), 1362–1369. MR798889 (87a:76058)
[17] M. R. Malik, *The neutral curve for stationary disturbances in rotating-disk flow*, J. Fluid Mech., **164** (1986), 275–287. MR844675 (87f:76113)
[18] L. M. Mack, *The wave pattern produced by a point source on a rotating-disk*, AIAA Journal, **0490** (1985).
[19] S. P. Wilkinson and M. R. Malik, *Stability experiments in rotating-disk flow*, AIAA Pap., **1760** (1983).
[20] S. P. Wilkinson and M. R. Malik, *Stability experiments in the flow over a rotating-disk*, AIAA Journal, **23** (1985), 588–595.
[21] R. Kobayashi, Y. Kohama and Ch. Takamadate, *Spiral vortices in boundary layer transition regime on a rotating-disk*, Acta Mech., **35** (1980), 71–82.
[22] A. J. Faller, *Instability and transition of disturbed flow over a rotating-disk*, J. Fluid Mech., **230** (1991), 245–269.
[23] B. I. Federov, G. Z. Plavnik, I. V. Prokhorov and L. G. Zhukhovitskii, *Transitional flow conditions on a rotating-disk*, J. Eng. Phys., **31** (1976), 1448–1453.
[24] P. Balakumar and M. R. Malik, *Travelling disturbances in rotating-disk flow*, Theoret. Comput. Fluid Dyn., **2** (1990), 125–137.
[25] K. Stewartson, *On the flow near the trailing-edge of a flat plate*, MATHEMATICA, **16** (1969), 106–121.
[26] K. Stewartson and P. G. Williams, *Self-induced separation*, Proc. Roy. Soc. London Ser. A, **312** (1969), 181–206.
[27] F. T. Smith, *On the high Reynolds number theory of laminar flows*, IMA Journal of Applied Mathematics, **28** (1982), 207–281. MR666155 (83g:76047)
[28] V. V. Sychev, A. I. Ruban, Vic. V. Sychev and G. L. Korolev, *Asymptotic theory of separated flows*, Cambridge University Press (1998). MR1659235 (2000d:76049)
[29] F. T. Smith, *On the non-parallel flow stability of the Blasius boundary layer*, Proc. Roy. Soc. London Ser. A, **366** (1979), 91–109.
[30] F. T. Smith and R. J. Bodonyi, *Nonlinear critical layers and their development in streaming flow stability*, J. Fluid Mech., **118** (1982), 165–185. MR663988 (83g:76055)
[31] P. Hall, *An asymptotic investigation of the stationary modes of instability of the boundary layer on a rotating-disk*, Proc. Roy. Soc. London Ser. A, **406** (1986), 93–106.
[32] A. P. Bassom and J. S. B. Gajjar, *Non-stationary crossflow vortices in a three dimensional boundary layer*, Proc. Roy. Soc. London Ser. A, **417** (1988), 179–212. MR944282 (89e:76036)
[33] M. Turkyilmazoglu and J. S. B. Gajjar, *Upper branch non-stationary modes of the boundary layer due to a rotating-disk*, Applied Mathematics Letters, **14** (2001), 685–690. MR1836070 (2002d:76050)
[34] Y. Kohama, *Crossflow instability in rotating-disk boundary layer*, AIAA Pap., **1340** (1987).
[35] Y. Kohama, *Crossflow instability in a spinning disk boundary layer*, AIAA Journal, **31** (1992), 212–214.
[36] S. O. Mackerrel, *A nonlinear asymptotic investigation of the stationary modes of instability of the 3 dimensional boundary layer on a rotating-disk*, Proc. Roy. Soc. London Ser. A, **413** (1987), 497–513. MR915128 (89a:76038)
[37] S. L. G. Jarre and M. P. Chauve, *Experimental study of rotating-disk instability. I. Natural flow*, Phys. Fluids, **8** (1996), 496–508.
[38] S. L. G. Jarre and M. P. Chauve, *Experimental study of rotating-disk instability. II. Forced flow*, Phys. Fluids, **8** (1996), 2985–2994.
[39] M. Turkyilmazoglu, *Lower branch modes of the compressible boundary layer flow due to a rotating-disk*, Stud. Appl. Maths., **114** (2005), 17–43. MR2117326 (2005h:76033)
[40] M. Turkyilmazoglu, *Non-linear and non-stationary modes of the lower branch of the incompressible boundary layer flow due to a rotating-disk*, Quart. Appl. Math., **65** (2007), 43–68. MR2313148

[41] K. Stewartson, *The theory of laminar boundary layers in compressible fluids*, Oxford University Press (1964).
[42] N. Riley, *The heat transfer from a rotating-disk*, Q. J. Mech. Appl. Math., **17** (1964), 331–349. MR0169488 (29:6736)
[43] M. Turkyilmazoglu and N. Uygun, *Compressible modes of the rotating disk boundary layer flow leading to absolute instability*, Stud. Appl. Maths., **115** (2005), 1–20. MR2141274 (2005m:76153)
[44] M. Abramowitz and I. A. Stegun, *Handbook of mathematical functions*, Dover Publications (1955).
[45] M. Turkyilmazoglu, *Effects of mass transfer on the non-stationary lower branch modes of a compressible boundary layer flow*, Stud. Appl. Maths., **115** (2005), 357–385. MR2172694 (2006e:76100)
[46] M. R. Dhanak, *Effects of uniform suction on the stability of flow on a rotating disc*, Proc. Roy. Soc. London Ser. A, **439** (1992), 431.